ISSN: 2579-5821 (Print)
ISSN: 2579-5546 (Online)
URL address: http://journal.unhas.ac.id/index.php/geocelebes
DOI: 10.20956/geocelebes.v8i1.32159

Jurnal Geocelebes Vol. 8 No. 1, April 2024, 62 – 70

Application of Seismic Refraction Tomography in Determining the Soil Hardness Level in IKN Nusantara Area

Andi Alamsyah, Piter Lepong, Wahidah*, Rahmiati

Geophysics Study Program, Mulawarman University, 75242, Indonesia.

*Corresponding author. Email: wahidah@fmipa.unmul.ac.id

Manuscript received: 5 December 2023; Received in revised form: 10 March 2024; Accepted: 27 April 2024

Abstract

Numerous studies supporting infrastructure construction are currently underway in the New Capital Territory of Nusantara (IKN Nusantara). A geophysical method known as Seismic Refraction Tomography (SRT) has been employed within the IKN Nusantara to identify hard and soft layers based on the P-wave velocity (Vp). The data acquisition involved 24 channels of geophone spaced at intervals 3 and 4 meters. Measurements were conducted alongfour trajectories of 69 and 92 meters, reaching penetration depths of 12 – 20 meters. P-wave velocity values ranging between 200 – 3500 m/s were recorded. Additionally, the Unconfined Compressive Strength (UCS) value was determined using an empirical equation tailored for mudrock-shale lithology, establishing the correlation between Vp and UCS. In the shallow depths of 0 – 3 meters, UCS values indicated levels below 20 MPa, classifying the materials as having low to medium hardness. However, at depths greater than 3 meters, this layer transitioned to material with high hardness levels, as evidenced by UCS rate exceeding 20 MPa across all trajectories. This suggest that the IKN Nusantara is conducive to infrastructure development.

Keywords: Infrastructure; New Capital Territory of Nusantara (IKN Nusantara); Seismic Refraction Tomography (SRT); Vp.

Citation: Alamsyah, A., Lepong, P., Wahidah, W., & Rahmiati, R. (2024). Application of Seismic Refraction Tomography in Determining the Soil Hardness Level in IKN Nusantara Area. *Jurnal Geocelebes*, 8(1): 62 – 70, doi: 10.20956/geocelebes.v8i1.32159

Introduction

East Kalimantan is the province where the capital of the new state (IKN Nusantara), exhibits diverse geological formations that fundamentally shape soil characteristics. These variations in the soil characteristics and geological structures significantly impact geotechnical properties, encompassing strength, consolidation, and drainability (Efendi, 2023). A comprehensive comprehension of these geotechnical aspects is imperative for the strategic planning of secure, sustainable development and the effective mitigation of potential disasters stemming from natural conditions natural conditions.

Bachtiar (2022) highlighted the prevalent geological structure in the IKN area, primarily characterized by NE-SW faults, as illustrated in Figure 1. Ezrahayu and Supriyanto (2021) also stated that the location of the prospective new national capital has structures in the form of anticlines, synclines, and is thought to contain thrust faults and normal faults. However, there is a lack of in-depth analysis and detailed studies on this aspect. Generally, regions with such fault structures are considered prone to landslide, a critical factor that demands thorough consideration during the construction-of future infrastructures for the area's development.

Seismic Refraction Tomography (SRT) has become a common method for exploring the geotechnical properties of soil (Asamoah et al., 2018; Whiteley et al.,

2018; Oladotun et al., 2019; Adewoyin et al., 2021; Shin et al., 2022; Opemipo et al., 2022; El Hameedy et al., 2023). According to Jabrane et al. (2023) and Abudeif et al. (2023), this technique relies on the principle of seismic wave retardation, which is dispersed by layers of rocks beneath the surface. This dispersion produces a representation of the variation in compressional wave velocity (P-wave velocity – Vp) within the earth.

This study focuses on assessing the hardness level of the soil beneath the IKN to support infrastructure development using the mentioned geophysical method.

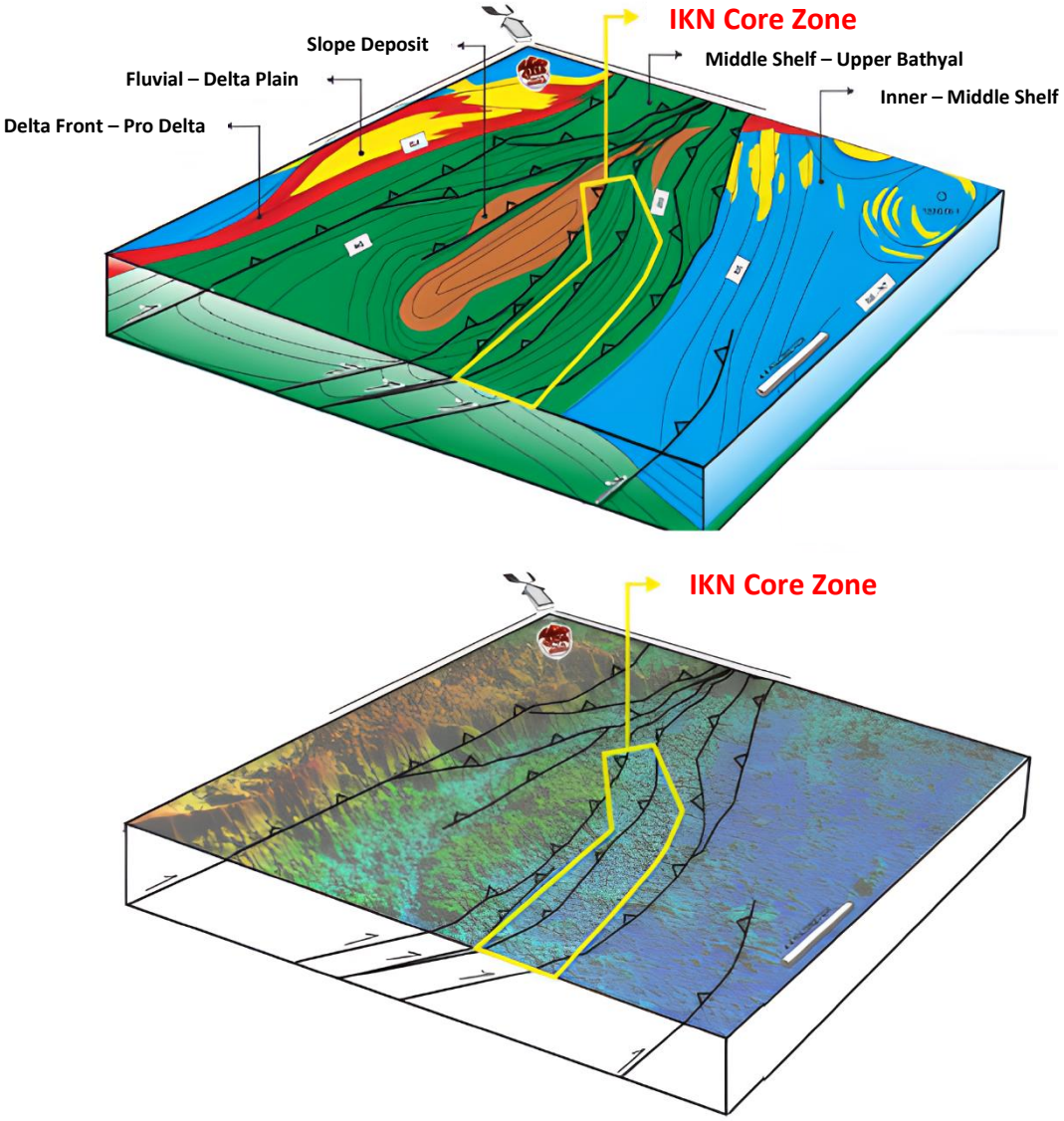

Figure 1. Fault interpretation in the facies of IKN area (Bachtiar, 2022).

Geological Background

Geologically, the location of this survey is included in the geological sheet of Balikpapan (Supriatna et al., 1995). The top formations consist of quartz brass with inserts of sludge, scraps, pebbles, and fine-layer oleic stones. Quartz brass is the main rock in this formation, which has a color range of green, gray, to brownish, fine to moderate grains. The Pamaluan Formation is the lowest rock found in the Samarinda sheet, and the upper part of the formation relates to the Bebulu Formation.

Stratigraphically, according to Bachtiar (2022), the geological composition of the study area is characterized by marine sediments attributed to the late Tertiary-Oligocene Pamaluan Formation, representing a middle shelf facies. This is illustrated in the stratigraphic column in Figure 2, with the IKN area highlighted by red boxes.

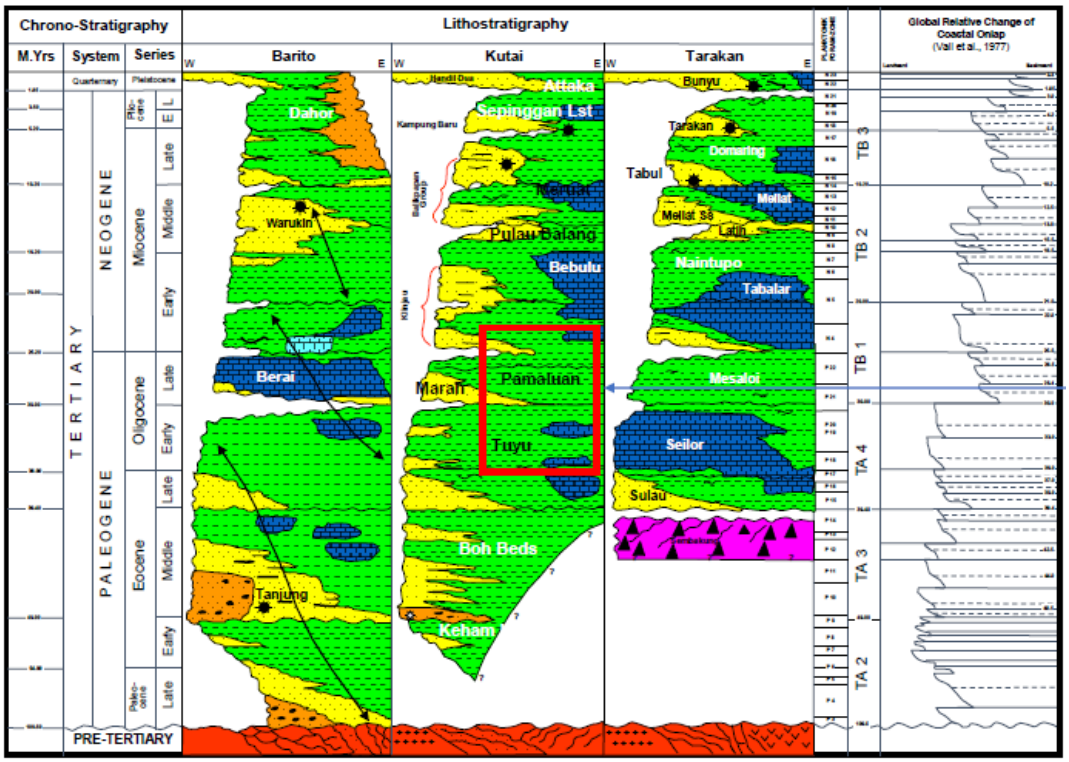

Figure 2. Stratigraphic chart of the regional geology of area (Bachtiar, 2022).

In particular, the research area is situated in the Sepaku District, Penajam North Paser Regency, East Kalimantan Province, precisely where the new state capital of Indonesia (IKN Nusantara area) is being developed, as illustrated in Figure 3.

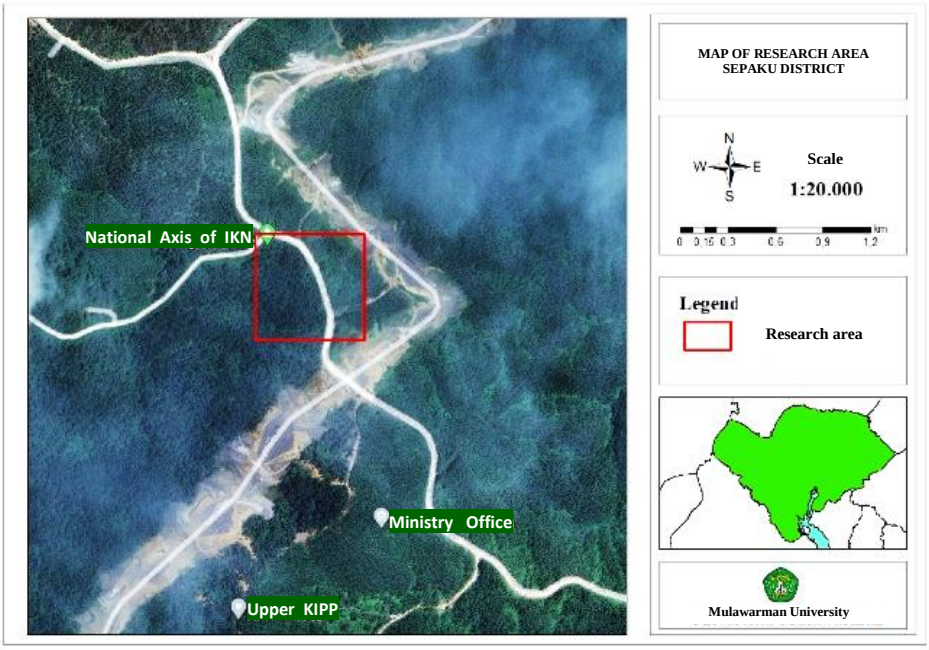

Figure 3. The map of the research area.

The study encompassed seismic refraction data acquisition, subsequent data processing, and interpretation. The acquisition phase utilized a DAQLink III seismograph equipped with 24 channels and a 9 kg hammer sledge serving as the wave source. A total of four seismic refraction surveys were carried out, with one track oriented NE-SW (parallel to the strike direction) and the remaining three tracks oriented relatively NW-SE (perpendicular to the strike). Track details are presented in Table 1 below.

Table 1. Track details.

Tracks	Geophone spacing (m)	Track length (m)
1 *(parallel to the strike)*	4	9
2	3	6
3	3	69
4	3	69

A simplified flow chart of this study is shown in the following Figure 4.

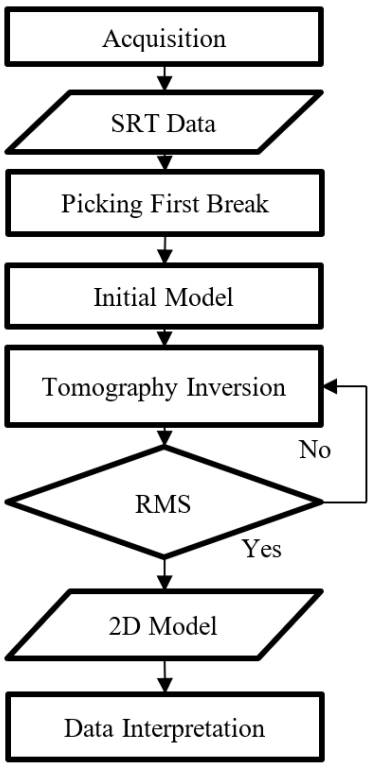

Figure 4. The map of the research area

1. **Picking First Break**. The timing of the wave is established by identifying the position of the first break on the refractive seismic record. The selection of the first break involves a subjective assessment to determine its position.
2. **Inversion Tomography**. This step involves generating a two-dimensional model of Vp intersections to illustrate subsurface conditions.
3. **Interpretation and 2D Model of Vp.** The Vp 2D model is scrutinized and interpreted by comparing the primary wave velocity (Vp) values with reference tables or previous research. Additionally, an analysis is conducted to assess the concordance of the interpreted primary wave velocity results with the geological conditions at the research site, enhancing the accuracy of the findings. Subsequently, the Vp values are incorporated into Equation 1.

$$UCS = 12.746 * Vp^{1.194} \quad (1)$$

This equation is an empirical relationship applicable to mudrock–shale rocks and siltstone or flax rocks (Poulos, 2021). The calculated results are employed to ascertain the hardness level or provide geotechnical descriptions, as outlined in Table 2.

Table 2. Relationship between Vp dan UCS (Poulos, 2021)

Vp (km/s)	Geotechnical Desc.	UCS (MPa)
< 2.0	Low strength rock	< 10
2.0 – 2.5	Medium strength rock	10 – 20
2.5 – 3.5	High strength rock; stratified, jointed	20 – 60
– 7.0	Very high strength rock	> 60

Results and Discussion

Seismic Refraction Tomography (SRT) cross-section on Track 1, Track 2, Track 3, and Track 4 are shown in Figure 5. The color bar in the figure represents the value

of the Vp, where the blue to red color shows the Vp from low to high.

Cross-section of Track 1, as depicted in Figure 5a, indicates the presence of two lithologies: soil and clay shale. Lithology 1 represents soil with a P-wave velocity ranging from approximately 700 to 1000 m/s and an average thickness of 2 meters. The soil near the surface is categorized as soft soil with a Vp around 700 to 800 m/s and a thickness of approximately 1 meter.

The undulation Vp contour lines indicate the heterogeneous presence of soil-containing material close to the surface. Between 50 and 80 meters, there is a change in the relative descent of the contour pattern, interpreted as subsidence or a decrease in seismic profiles.

In general, higher Vp values correspond to materials with greater geotechnical strength due to increased density, while porosity, weathering, and fracturing decrease. The Vp values can be utilized to calculate the Ultimate Compressive Strength (UCS). In Track 1, the predominant lithology falls into the high-strength rock category, with a calculated UCS ranging from 22 to 51 MPa. Conversely, the soil near the surface is classified as low to medium strength rock, with a UCS value less than 15.85 MPa.

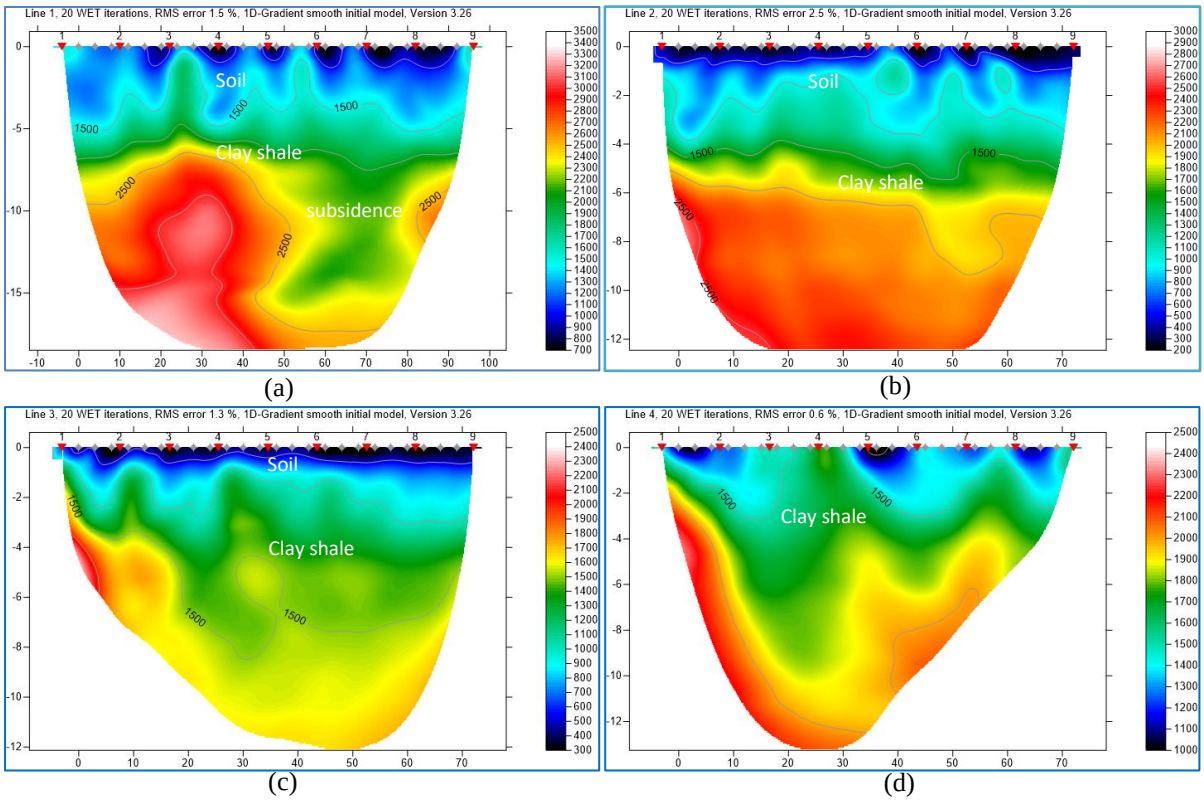

Figure 5. SRT (Vp) section of (a) Track 1; (b) Track 2; (c) Track 3; (d) Track 4.

Track 2, oriented perpendicular to the strike (NW-SE), exhibits two distinguishable lithologies: soil and clay shale. The soil layer is characterized by a Vp ranging from approximately 200 to 1000 m/s, with an average thickness of 3 meters.

The surface soil, with a Vp of around 200 to 800 m/s, is interpreted as soft soil and has a thickness of approximately 1 meter. Additionally, lithology 2 is identified as clay shale, featuring a Vp between 1000 and 3500 m/s and located at a depth of 3 to 12 meters.

In Figure 5b, the undulation Vp contour lines indicate the presence of inhomogeneous material, particularly soil

close to the surface. At a depth greater than 4 meters, where Vp exceeds 1500 m/s, the clay shale layering pattern appears relatively uniform. This is interpreted as a relatively stable stratum without structural features such as fractures or faults.

The cross-section of Track 2 is predominantly classified as medium-high strength rock category with UCS calculation resulting in a range of (19-38) MPa. The surface soil falls into the low strength rock category, with a UCS value of less than 6 MPa.

Moreover, track 3 exhibits a lithology pattern similar to the preceding tracks. The soil layer has a Vp ranging from approximately 300 to 1000 m/s with an average thickness of 2 meters. The surface soil, with a Vp of around 200 to 800 m/s, is interpreted as soft soil with a thickness of approximately 1 meter. The second lithology is identified as clay shale, featuring a Vp between 1000 and 3500 m/s, located at a depth of 3 to 12 meters. The depth of the clay shale layer on this track is roughly the same as the one found on Track 2.

The undulation of the Vp contour lines reveals in homogeneous especially soil close to the surface. At depths exceeding8 meters with Vp >1500m/s, it is observed that the clay shale bedding pattern is relatively deeper compared to other tracks. These results, suggest that the clay shale is relatively tilted to the west.

Overall, the dominant section of Track 3 falls into the high-strength rock category, with UCS calculation results ranging from (20-22) MPa. The surface soil is categorized as low-strength rock, with a UCS value of less than 10 MPa. In Track 4, which is aligned with the dip direction, only one lithology has been identified, which is clay shale, as illustrated in Figure 5d. The topsoil layer was not discernible as it had been removed in this area. The clay shale layer on this track exhibits a Vp ranging from approximately 1000 to 2500 m/s, extending from the surface to a depth of 12 meters. The undulating Vp contour lines indicate the presence of material inhomogeneity, particularly soil close to the surface. The undulating velocity contour pattern is attributed not only to the inhomogeneity of the clay shale material but also to the influence of noise generated by the vibrational activity of heavy equipment actively operating in the survey area.

On the other hand, the cross-section of Track 4 is predominantly classified as high-strength rock, with UCS calculation results ranging from (24-31) MPa. The surface soil falls into the medium-strength rock category, with a UCS value of less than 18 MPa. The UCS calculation results using Equation 1 are presented in Table 3, which also provides a geotechnical description based on the correlation results of Vp with UCS.

Generally, the P wave velocity values from the results of seismic refraction tomography (SRT) measurements on the four tracks show two lithologies, namely soil with a Vp value of around 200 m/s - 1000 m/s and clay shale with a Vp value of around 1000 m/s - 3500 m/s, except for Track 4, only the clay shale layer was identified and exposed on the surface. In civil construction terms, clay shale is classified as an intermediate rock containing montmorillonite clay (Ohlmacher, 2000; Akisanmi 2022).

Its presence poses a challenge because of its low durability making it susceptible to weathering (Pratama et al., 2015). Therefore, special attention is needed in civil construction planning to overcome this factor.

Even though the research area is dominated by clay shale lithology, the level of rock strength also needs to be considered to determine whether construction is feasible in the area. Based on Table 3, the average

UCS value of the four tracks is greater than 20 MPa which is categorized as high strength rock geotechnical material, except for soil material close to the surface to a depth of around 3 meters which is categorized as low to medium strength rock.

Tanjung et al. (2023) and Amran and Pradana (2023) claim that properly compacted clay soil will have increased shear strength. The mineral content of the material determines how stable its swelling-shrinking characteristics are.

This is supported by the results of research by Susilawati (2022) which states that measuring the strength of soil and rock by cone penetration test shows the presence of a hard layer (Qc >150 kg/cm^2) range between 2.0 – 4.0 m below the ground surface and locally can reaches 5.8 m.

Table 3. UCS calculation results with geotechnical description.

Track	Depth (m)	Vp (m/s)	UCS (MPa)	Geotechnical Description
1	0 – 2.5	1200	15.8	Medium Strength Rock
	2.5 - 6	1600	22.3	High Strength Rock
	6 – 10.5	2200	32.7	High Strength Rock
	10.5 - 16	2800	43.6	High Strength Rock
	16 -20	3200	51.1	High Strength Rock
2	0 – 2.5	500	5.6	Low Strength Rock
	2.5 - 6	1400	19.0	Medium Strength Rock
	6 – 10.5	2250	33.6	High Strength Rock
	10.5 - 12	2500	38.1	High Strength Rock
3	0 – 3	800	9.8	Low Strength Rock
	3 – 7.5	1500	20.7	High Strength Rock
	7.5 - 12	1600	22.3	High Strength Rock
4	0 – 2.5	1300	17.4	Medium Strength Rock
	2.5 - 6	1700	24.0	High Strength Rock
	6 – 10.5	1950	28.3	High Strength Rock
	10.5 - 13	2150	31.8	High Strength Rock

Table 3 shows a correlation between the P wave velocity value and the UCS value. According to Awang et al. (2017) and Kessler et al. (2017), it is now simpler to determine UCS value without the necessity for physical testing on samples or borehole and sample collection processes because this empirical link has been acknowledged. We are able to recognize that the compressive strength index value is crucial for the design factor because of the seismic test that yields the P-wave velocity value when conducted on the ground surface. One of the most crucial factors in rock engineering qualities is the UCS value.

In civil construction terms, clay shale is classified as an intermediate rock containing montmorillonite clay that has low durability due to weathering. Hence, special attention is required in civil construction planning to address this factor. However, the average UCS value of clay lithology at a depth of more than 3 meters is still considered suitable for construction because it is still greater than 20 MPa which is categorized as high strength rock geotechnical material. To be more convincing, it is necessary to carry out a MASW (Multichannel Analysis Surface Wave) survey to analyze the level of rock stiffness and other geotechnical parameters.

Conclusion

The Seismic Refraction Tomography (SRT) measurements reveal that the predominant compression seismic wave velocity (Vp) exceeds 1500 m/s interpreted as clay shale which is under the soil layer.

Acknowledgements

The authors acknowledged the Head of Geophysics Laboratory for supporting the SRT tools and FMIPA UNMUL for funding this research.

Author Contribution

Field acquisitions were carried by Piter Lepong and Team. All authors discussed, interpreted and wrote the manuscripts which were leading by Andi Alamsyah.

Conflict of Interest

The authors declare no conflict of interest.

References

Abudeif, A. M., Aal, G. Z. A., Abdelbaky, N. F., Gowad, A. M. A., & Mohammed, M. A. (2023). Evaluation of Engineering Site and Subsurface Structures Using Seismic Refraction Tomography: A Case Study of Abydos Site, Sohag Governorate, Egypt. *Applied Sciences*, 13(4), 2745. https://doi.org/10.3390/app13042745

Adewoyin, O. O., Joshua, E. O., Akinyemi, M. L., Omeje, M., & Adagunodo, T. A. (2021). Evaluation of Geotechnical Parameters of Reclaimed Land from Near-Surface Seismic Refraction Method. Heliyon, 7(4), E06765. https://doi.org/10.1016/j.heliyon.2021.e06765

Akisanmi, P. (2022). Classification of Clay Minerals. *Mineralogy* (M. René (ed.); p. Ch. 12). IntechOpen. https://doi.org/10.5772/intechopen.103841

Amran, Y., & Pradana, D. Y. (2023). Parameter Nilai Kuat Tekan Bebas Tanah terhadap Tingkat Kepadatan Tanah Lempung Ekspansif. *Teknologi Aplikasi Konstruksi (TAPAK)*, 12(2), 166–178. http://dx.doi.org/10.24127/tp.v12i2.2595

Asamoah, K. N., Seidu, J., Ewusi, A., & Ansah, E. (2018). Geotechnical Investigation at Sanzule Beach, Ghana, Using Seismic Refraction Tomography. *IJISET-International Journal of Innovative Science, Engineering & Technology*, 5(2), 45–53. https://ijiset.com/vol5/v5s2/IJISET_V5_I02_05.pdf

Awang, H., Rashidi, N.R.A., Yusof, M., & Muhammad, K. (2017). Correlation Between P-wave Velocity and Strength Index for Shale to Predict Uniaxial Compressive Strength Value. *MATEC Web of Conferences* 103, 07017. https://doi.org/10.1051/matecconf/201710307017

Bachtiar, A. (2022). *Aspek geologi untuk mitigasi bencana Ibu Kota Nusantara*. National Webinar. https://www.its.ac.id/tgeofisika/wp-content/uploads/sites/33/2022/11/Materi-Dr-Andang-Bachtiar.pdf

Efendi, A. W. (2023). Pemodelan Penurunan Tanah Di Ibu Kota Negara Nusantara Menggunakan Analisis Numerik Metode Elemen Hingga Lisa V.8. *Paduraksa: Jurnal Teknik Sipil Universitas Warmadewa*, 12(1), 21–29. https://doi.org/10.22225/pd.12.1.5643.21-29

El Hameedy, M. A., Mabrouk, W. M., Dahroug, S., Youssef, M. S., & Metwally, A. M. (2023). Role of Seismic Refraction Tomography (SRT) in bedrock mapping; case study from industrial zone, Ain-Sokhna area, Egypt. *Contributions to Geophysics and Geodesy*, 53(2), 111–128. https://doi.org/10.31577/congeo.2023.53.2.2

Ezrahayu, P. & Supriyanto, S. (2021). Identifikasi Sesar di Bawah Permukaan yang Dapat Menyebabkan Gempa Berdasarkan Metode First Horizontal Derivative dan Second Vertical Derivative di Kabupaten Penajam Paser Utara, Kalimantan Timur. *Jurnal Geosains Terapan* 4(1), 15–22. https://geosainsterapan.id/index.php/id/issue/download/6/6

Jabrane, O., Martinez-Pagan, P., Martinez-Segura, M. A., Alcala, F. J., El Azzab,

D., Vásconez-Maza, M. D., & Charroud, M. (2023). Integration of Electrical Resistivity Tomography and Seismic Refraction Tomography to Investigate Subsiding Sinkholes in Karst Areas. *Water*. 15(12), 2192. https://doi.org/10.3390/w15122192

Kessler, J. A., Schmitt, D.R., Chen, X., Evans, J. P., & Shervains, J. W.. (2017). Predicting Uniaxial Compressive Strength from Empirical Relationships between Ultrasonic P wave Velocities, Porosity, and Core Measurements in a Potential Geothermal Reservoir, Snake River Plain, Idaho. *American Rock Mechanics Association (ARMA)*, 17-391. https://www.osti.gov/servlets/purl/1749943

Ohlmacher, G. C. (2000). The Relationship Between Geology and Landslide Hazards of Atchison, Kansas, and Vicinity. *Current Research in Earth Science,* 244, 1–16. https://doi.org/10.17161/cres.v0i244.11833

Oladotun, A. O., Oluwagbemi, J. E., Lola, A. M., Maxwell, O., & Sayo, A. (2019). Predicting Dynamic Geotechnical Parameters in Near-Surface Coastal Environment. *Cogent Engineering*, 6(1), 1588081. https://doi.org/10.1080/23311916.2019.1588081

Opemipo, O. D., Moroff, O., Sunday, O., Victor, O., & Christopher, B. (2022). Subgrade Soil Evaluation Using Integrated Seismic Refraction Tomography and Geotechnical Studies: A Case of Ajaokuta-Anyigba Federal Highway, North-Central Nigeria. *NRIAG Journal of Astronomy and Geophysics*, 11(1), 293–305. https://doi.org/10.1080/20909977.2022.2094530

Pratama, A. W., Iswan, I., & Jafri, M. (2015). Korelasi Kuat Tekan dengan Kuat Geser pada Tanah Lempung yang Didistribusi dengan Variasi Campuran Pasir. *Journal Rekayasa Sipil Dan Desain (JRSDD)*, 3(1), 157–170. https://journal.eng.unila.ac.id/index.php/jrsdd/article/view/434

Poulos, H. G. (2021). Use of shear wave velocity for foundation design. *Geotechnical and Geological Engineering*, 40(2), 1921–1938. https://doi.org/10.1007/s10706-021-02000-w

Shin, B.-S., Wientgens, L., Schaab, M., & Shutin, D. (2022). Near-Surface Seismic Measurements in Gravel Pit, over Highway Tunnel and Underground Tubes with Ground Truth Information as an Open Data Set. *Sensors*, 22(17), 6687. https://doi.org/10.3390/s22176687

Supriatna, S. Sukardi, R, & R. Rustandi. (1995). *Peta Geologi Bersistem, Lembar Samarinda, Kalimantan skala 1:250.000*. Pusat Penelitian dan Pengembangan Geologi.

Susilawati, R. (2022). *Kajian geologi dalam rencana pembangunan IKN nusantara*. Diskusi IAGI "Menyongsong IKN Nusantara dari Perspektif Kebumian". https://www.iagi.or.id/web/digital/43/Hasil-Kajian-Geologi-dalam-Rencana-Pembangunan-IKN-Nusantara-(1).pdf

Tanjung, D., Sarifah, J., & Ardian, J. P. (2023). Pengaruh Nilai Kuat Tekan Bebas terhadap Penambahan Abu Sekam Padi pada Tanah Lempung. *Jurnal Teknik Sipil*. 2(1), 68–77. https://jurnal.uisu.ac.id/index.php/JTSIP/article/view/7662

Whiteley, J. S., Chambers, J. E., Uhlemann, S., Wilkinson, P. B., & Kendall, J. M. (2018). Geophysical Monitoring of Moisture-Induced Landslides: A Review. *Review of Geophysics*, 57(1), 106–145. https://doi.org/10.1029/2018RG000603